



Fraunhofer Institut
Bauphysik

Bauaufsichtlich anerkannte Stelle
für Prüfung, Überwachung und
Zertifizierung
Zulassung neuer Baustoffe, Bauteile
und Bauarten
Forschung, Entwicklung,
Demonstration und Beratung auf
den Gebieten der Bauphysik

Institutsleitung
Prof. Dr. Gerd Hauser
Prof. Dr. Klaus Sedlbauer

Description of the IBP holistic hygrothermal model

Andreas Holm
Jan Radon
Hartwig Künzle
Klaus Sedlbauer

Holzkirchen, 22. April 2004

Description of the IBP holistic hygrothermal model

1	Introduction	3
2	Combining thermal building simulation and hygrothermal envelope calculation	3
2.1	Governing equations for the hygrothermal envelope calculation	4
2.2	Governing equations of the hygrothermal whole building simulation model	5
3	Comparison with other Models	7
4	Experimental validation	10
5	Results	12
6	Model application	14

1 Introduction

During the last years several models for calculating the thermal behavior of a building were developed. The application of programs like ESP-r, TRNSYS, DOE-2 and EnergyPlus is a standard for designer. A good overview of building simulation tools can be found on the webpage of U.S. Department of Energy (http://www.eren.doe.gov/buildings/tools_directory).

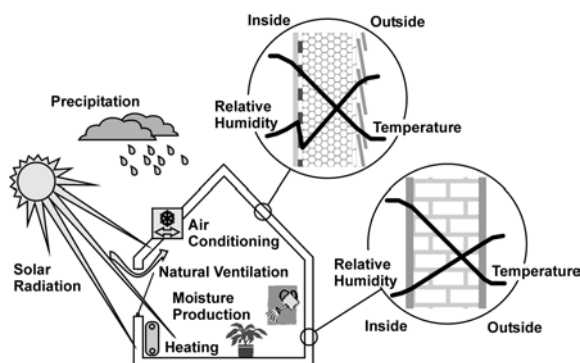
Nevertheless, most of the commonly used thermal building simulation tools treat the moisture exchange with the envelope in a simplified manner by assigning a certain moisture storage capacity to the interior of the building. This approach is often sufficient as long as average humidity conditions are the only concern. However, if the exact indoor humidity fluctuations or the moisture profiles in the building envelope are relevant new models that combine the thermal building simulation with the hygrothermal component simulation have to be developed.

In this paper a hygrothermal whole building simulation model and its validation will be presented. The model takes into account the main hygrothermal effects, like moisture sources and sinks inside a room, moisture input from the envelope due to capillary action, diffusion and vapour ab- and desorption as a response to the exterior and interior climate conditions, heat sources and sinks inside the room, heat input from the envelope, the solar energy input through walls and windows and hygrothermal sources and sinks due to natural or mechanical ventilation.

2 Combining thermal building simulation and hygrothermal envelope calculation

As mentioned before there are a number of validated models for thermal building simulations as well as hygrothermal envelope calculations used in building practice today. However, working combinations of these models are not yet available for the practitioner. In principle, this combination is done by coupling existing models of both types. Figure 1 shows the concept of such a combination where balance equations for the interior space and the different envelope parts have to be solved simultaneously. Recently the first real hygrothermal simulation models have been developed [Karagiozis et al. 2001, Rode et al. 2001] but so far only limited validation cases have been reported. The model employed in this paper is called WUFI®Plus [Holm et al. 2002] and is based on the hygrothermal envelope calculation model WUFI® [Künzel 1994].

Figure 1: Coupling concept for the simultaneous treatment of the hygrothermal effects of interior heat and moisture loads, exterior climate and transient behavior of envelope components.



2.1 Governing equations for the hygrothermal envelope calculation

For the coupled heat and mass transfer for vapor diffusion, liquid flow and thermal transport in the envelope parts the model solves the following equations

Energy conservation

$$\left(\rho c + \frac{\partial H_w}{\partial \theta} \right) \cdot \frac{\partial \theta}{\partial t} = \nabla \cdot (\lambda \nabla \theta) + h_v \nabla \cdot (\delta_p \nabla (\phi p_{sat})) \quad (1)$$

Mass conservation

$$\frac{dw}{d\phi} \cdot \frac{\partial \phi}{\partial t} = \nabla \cdot \left(D_w \frac{dw}{d\phi} \nabla \phi + \delta_p \nabla (\phi p_{sat}) \right) \quad (2)$$

where:

- ϕ = relative humidity, [-]
- t = time, [s]
- θ = temperature, [K]
- c = specific heat, [J/kgK]
- w = moisture content, [kg/m³]
- p_{sat} = saturation vapour pressure, [Pa]
- λ = thermal conductivity, [W/(mK)]
- H = total enthalpy, [J/m³]
- D_w = liquid diffusivity, [m²/s]
- δ_p = vapour permeability, [kg/(msPa)]
- h_v = latent heat of phase change, [J/kg]

On the left-hand side of equation (1) and (2) are the storage terms. The fluxes on the right-hand side in both equations depend on local temperature and humidity conditions. The conductive heat flux and the enthalpy flux by vapor diffusion with phase changes in the energy equation are strongly depending on the moisture fields resp. fluxes. The liquid flux in the moisture transport equation is only slightly influenced by the temperature effect on the liquid

viscosity and consequently on D_ϕ . The vapour flux, however, is simultaneously governed by the temperature and moisture field due to the exponential changes of the saturation vapor pressure with temperature. Due to this close coupling and the strong non-linearity of both transport equations a stable and efficient numerical solver had to be designed for their solution.

The discretization of the transport equations is done by a fully implicit finite volume scheme with variable grid spacing. In the one-dimensional case this leads to difference equations which can be solved efficiently by the Thomas algorithm for tridiagonal matrices. The coupling of the discretized equations is assured by iterative consecutive solution of these equations using under-relaxation factors adapted to the progress of solution. Special care had to be taken formulating the difference equations containing the vapour pressure which is a function of the two transport variables temperature and relative humidity.

2.2 Governing equations of the hygrothermal whole building simulation model

Equations (1) and (2) must be solved for every part of the envelope individually. Beside the exact definition of the assembly, including the material properties, the corresponding interior and exterior climatic boundary conditions are required. Usually the exterior boundary conditions are hardly affected by the building. However, the interior climate conditions depend on several parameters, e.g. exterior climate, HVAC system, occupants' behaviour, humidity buffering of interior walls and furniture.

Heat balance of the room:

Due to the fact that energy simulations are widely used the thermal governing equations will not be explained in detail. The indoor room temperature θ_i is linked to the heat fluxes into the room. This means that not only the heat flux over the envelope (transmission and solar input) is important. In addition, internal thermal loads and the air exchange due to natural convection or HVAC systems must be taken into account. The energy balance can be described with the following equation.

$$\rho \cdot c \cdot V \cdot \frac{d\theta_i}{dt} = \sum_j A_j \alpha_j (\theta_j - \theta_i) + \dot{Q}_{Sol} + \dot{Q}_{i1} + n \cdot V \cdot \rho \cdot c \cdot (\theta_a - \theta_i) + \dot{Q}_{vent} \quad (3)$$

where:

- ρ = density of the air, [kg/m³]
- α_j = heat transfer coefficients [W/m²K]
- θ_a = exterior air temperature, [K]
- θ_j = surface temperature, [K]
- θ_i = indoor air temperature, [K]
- t = time, [s]
- A_j = surface area, [m²]

- c = heat capacity of the air [J/kgK]
- n = air change per hour, [h⁻¹]
- \dot{Q}_{sol} = solar input which leads directly to an increase of the air temperature or furniture, [W]
- \dot{Q}_{il} = internal gains such as people, lights and equipment, [W]
- $\dot{Q}_{vent.}$ = heat fluxes gained or lost due to ventilation, [W]
- V = volume, [m³]

Moisture balance of the room:

The moisture condition in the room are a consequence of the moisture fluxes over the interior surfaces, the user dependent moisture production rate and the gains or loses due to air infiltration, natural or mechanical ventilation as well as sources or sinks due to HVAC systems.

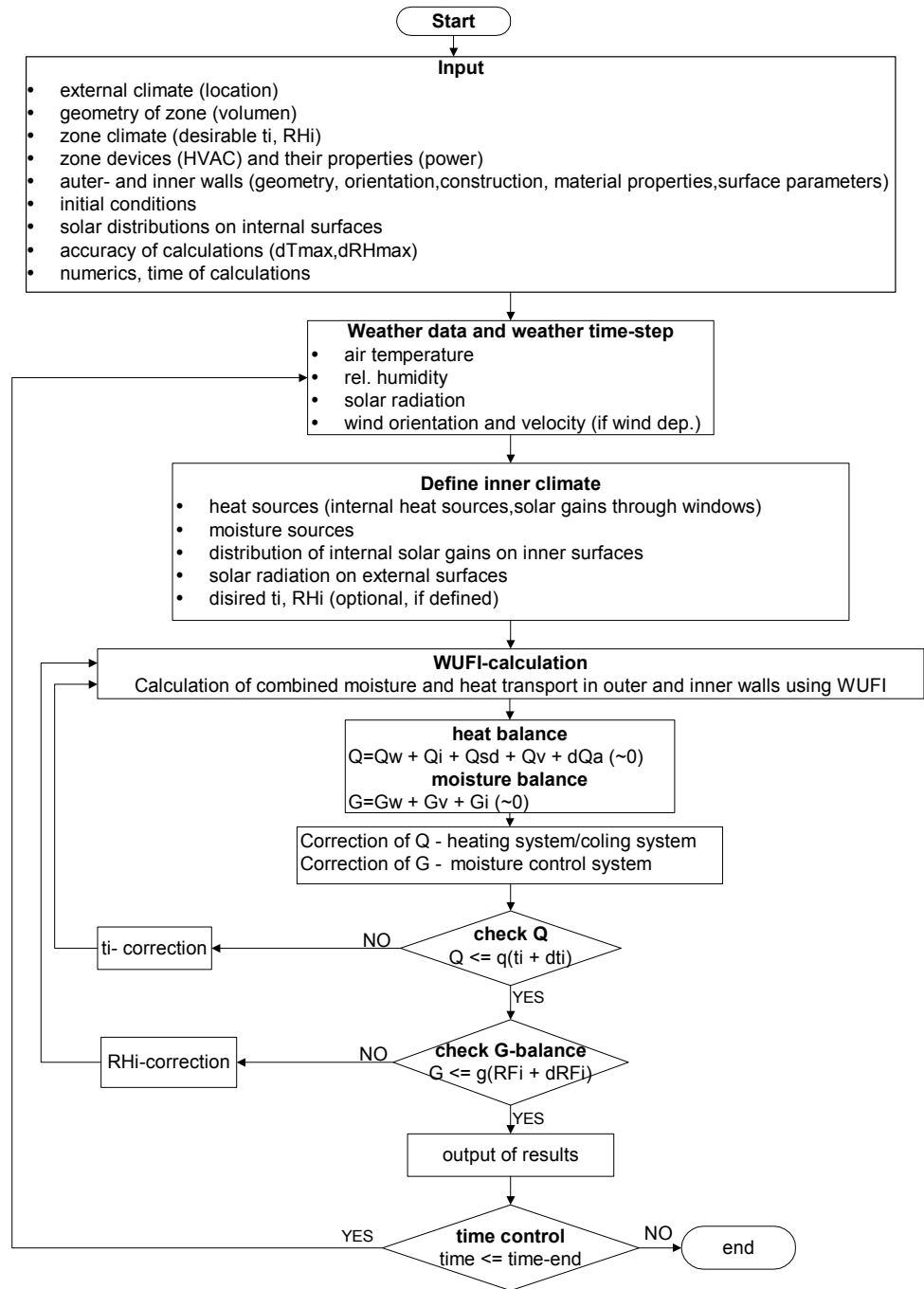
$$V \cdot \frac{dc_i}{dt} = \sum_j A_j \dot{g}_{w_j} + n \cdot V (c_a - c_i) + \dot{W}_{IMP} + \dot{W}_{vent} + \dot{W}_{HVAC} \quad (4)$$

where:

- c_a = absolute moisture ratio of the exterior air, kg/m³
- c_i = absolute moisture ratio of the interior air, kg/m³
- \dot{g}_{w_j} = moisture flux from the interior surface into the room, kg/(sm²)
- \dot{W}_{IMP} = moisture production, kg/h
- \dot{W}_{vent} = moisture gains or loses due to ventilation, kg/h
- \dot{W}_{HVAC} = moisture gains or loses due to the HVAC system, kg/h.

For each part of the envelope, the surface temperatures and moisture conditions, respectively the surface thermal and moisture fluxes are solved using equations (1) and (2). The required indoor conditions can be derived from equation (3) and (4). Because of the strong coupling of the two sets of equations the resulting indoor room temperature and relative humidity are determined iteratively. *Figure 2* shows the flow chart of the holistic approach.

Figure 2: Flow chart of WUFI®Plus



3 Comparison with other Models

For a typical application case, the results from WUFI®Plus with those from TRNSYS will be compared. Therefore, the thermal behavior of a two-story building made out of prefabricated AAC elements will be simulated. It is

assumed that the air exchange within the building is perfect and therefore the whole building can be simulated with a one-zone model.

The building with height of 6.5 m and 1625 m³ volume has a length of 20 m in east-west orientation and 12.5 m in north-south orientation. The building is designed without a basement. The flat roof is made out of concrete with a 180 mm thick insulation layer. The façade elements are made out of 36.5 cm thick AAC block work with an exterior mineral stucco and a gypsum plaster on the interior surface. On the south orientated façade 50 m² of windows are integrated, 20 m² on the other three facades. The U_w -value of the windows is assumed to be 1.4 W/(m²K) with a the total solar energy transmittance of 0.56. *Table 1* shows for all building parts the geometrical set-up. The material properties are taken from the WUFI® database [Künzel et al. 2001].

Table 1: geometrical setup of the building

	area [m ²]	assembly
exterior facade	S: 80 N: 110 W: 61,25 E: 61,25	-20 mm mineral stucco (water repellent, s_d -value: 0,2 m) -365 mm AAC -15 mm gypsum plaster
windows	S: 50 N: 20 W: 20 E: 20	-u-value: 1.4 W/mK -total solar energy transmittance: 0.56 -framing: 15 %
flat roof	250	-gravel -180 mm insulation -roof membrane V13 -200 mm concrete -15 mm gypsum plaster
floor	250	-60 mm cement screed -80 mm insulation -bituminous seal -160 mm concrete
ceiling	250	-60 mm cement screed -30 mm insulation -180 mm concrete -15 mm gypsum plaster
supporting wall	100	-15 mm gypsum plaster -150 mm concrete -15 mm gypsum plaster
room dividing wall	160	-20 mm gypsum board -50 mm mineral wool -40 mm air layer -20 mm gypsum board

The starting point is the beginning of the year with an initial moisture content corresponding to 80 % relative humidity. The hygrothermal behaviour is simulated over a period of one year. Hourly weather data measured in a typical year in Holzkirchen represent the climatic conditions. The infiltration rate is described with a constant ACH of 0.3 h⁻¹. The daily schedule of the moisture production rate can be seen in *Figure 3*. The total thermal load per hour is

1.2 kW. The comfort range for the interior humidity lies between 40 and 60 % RH with a maximum temperature of 27 °C.

Figure 3: Daily time schedule of the moisture production rate in the test rooms.

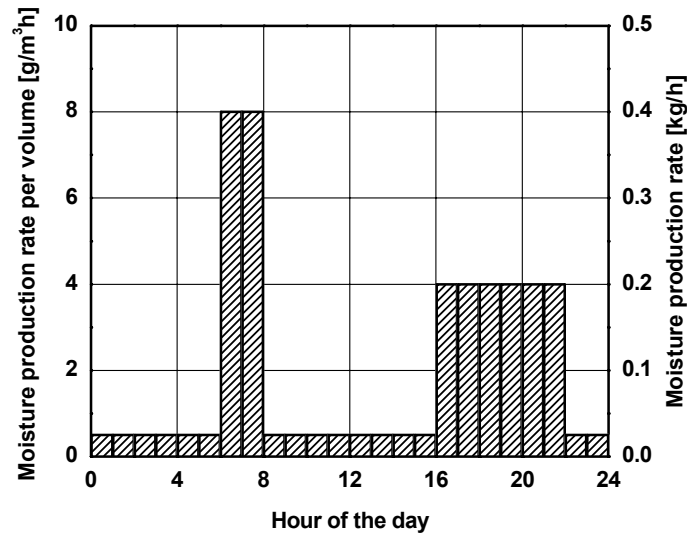
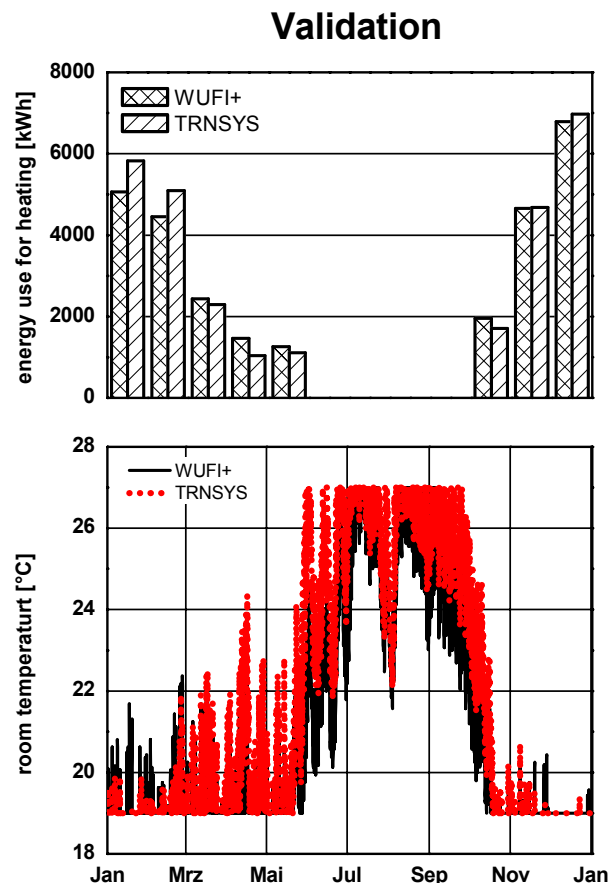


Figure 4 shows the direct comparison of the calculated energy for heating and the resulting room temperature. The results from WUFI®Plus and TRNSYS corresponds well. The total energy use for heating computed by WUFI®Plus is amount to 56 kWh/m²a which is only ca. 2 % below the result from TRNSYS. This minor deviation is considered acceptable for such calculations according to [VDI 2001, Gertis et al. 1988, Stricker et al. 1989].

Figure 4: WUFI®Plus and TRNSYS calculated energy use for heating and the resulting room temperature.



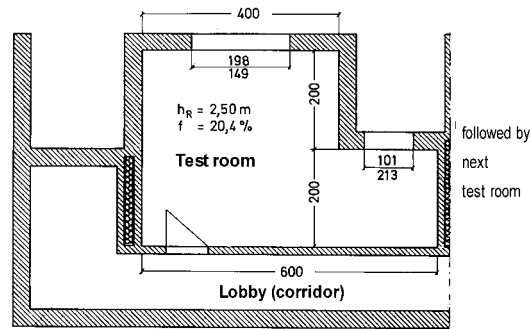
So far only the thermal part of it has been validated by comparing its results with those of well-established building simulation tools, but an important issue is the validation of these models by real life experiments carried out under well defined boundary conditions. The validation of the hygric part will be done within the frame of the experiments described below.

4 Experimental validation

The experiments are carried out in a building erected on the IBP test site in the 80s designed for energetic investigations published in [Künzel 1984]. Two of the five test rooms can be used for our purpose because they have identical walls. The ground plan of the test rooms and the adjacent spaces is plotted in *Figure 5*. The test rooms have a ground area of 20 m² and a volume of 50 m³. They are heavily insulated (200 mm of polystyrene) towards the ground. In order to avoid moisture flow to or from the ground the floor has a vinyl covering. The outer surfaces of the ceiling and interior wall sections are surrounded by a conditioned space. The external walls consist of 240 mm thick brick masonry with 100 mm exterior insulation (ETICS/EIFS). On the interior surface 12 mm of standard plaster is applied. The double-glazed windows are

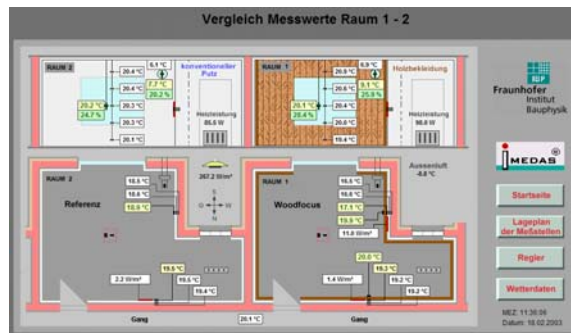
facing south (U-value: 1.1 W/mK, total solar energy transmittance: 0.57, frame ratio: 30 %). Special considerations is given to the air tightness of the rooms. Blower-door tests confirm a n_{50} value below 1 h^{-1} . Following IBP-investigations in the past reported in [Hens 1995] the walls and ceiling of one room (test room) is covered with aluminum foil while the other room is left as it is (reference room). Since the envelope of the test room has almost no sorption capacity it can be used to determine the moisture buffering effect of furniture and especially devised sorptive building components. The reference room with its plastered walls serves as an example for a typical construction of German houses.

Figure 5: Ground plan of the test room.



The rooms are equipped with calibrated heating, ventilation and moisture production systems as well as fans in order to avoid stratification. The indoor air temperature and humidity is measured at different levels above the ground. Temperature sensors and heat flux meters are also fixed to the interior surface of external walls. All values are measured on a five minute basis and can be analyzed with an internet-based tool developed by IBP called IMEDAS® (see Figure 6).

Figure 6: Screen shot of the internet-based visualization tool IMEDAS



The first tests are done with a constant air change rate of 0.5 h^{-1} which is the hygienic minimum rate according to German regulations. The indoor air temperature will also be kept constant at 20 °C controlled by a sensor in the middle of the room. The moisture production is derived from an average moisture load of 4 g/m^3 . This means the total amount of water dissipated in the room per day is 2.4 kg or 48 g/m^3 . In reality the production rate will not be constant over the whole day. Here a basic production rate of $0.5 \text{ g/m}^3\text{h}$ is

assumed with peaks in the morning and in the evening, i.e. $8 \text{ g/m}^3\text{h}$ from 6⁰⁰ to 8⁰⁰ a.m. and $4 \text{ g/m}^3\text{h}$ from 4⁰⁰ to 10⁰⁰ p.m. every day.

5 Results

The measured and calculated evolutions of the relative humidity in the empty test room during a day in January are plotted in *Figure 8*. The corresponding calculations are based on the assumptions as described above concerning indoor temperature, moisture production and ventilation. They are carried out for the test room in its original form (i.e. covered with aluminum) and the reference room, which is lined with the standard gypsum plaster. Since the outdoor climate has been rather constant for some time and the moisture production and ventilation pattern of the room are repeated every day, it is assumed that a dynamic equilibrium has evolved in the room. Therefore the RH of the indoor air at the end of the day is the same as at the beginning. There is a perfect agreement between experiment and numerical simulation. The humidity fluctuations are greatest during the peak load in the morning where the indoor humidity rises from 35% to over 80% which represents an increase of nearly 50% RH. (*Figure 8*)

Figure 7: Measured relative humidity inside the two test rooms.

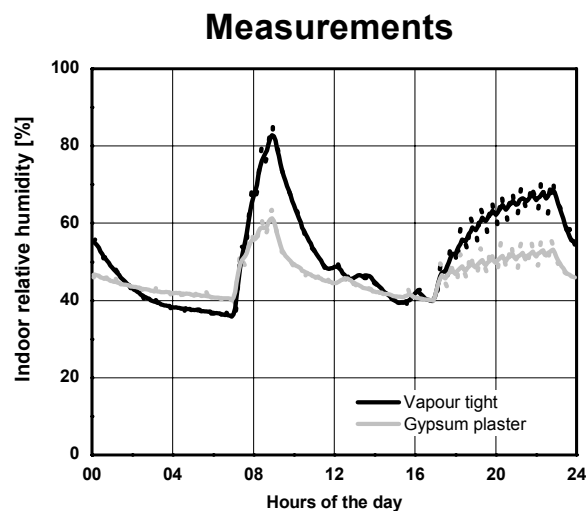


Figure 8: Simulated and measured evolution of the indoor air humidity during a diurnal cycle in the test room coated with aluminium foil.

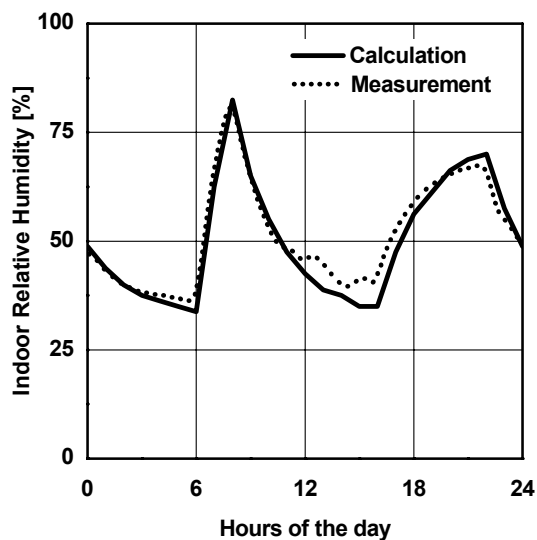
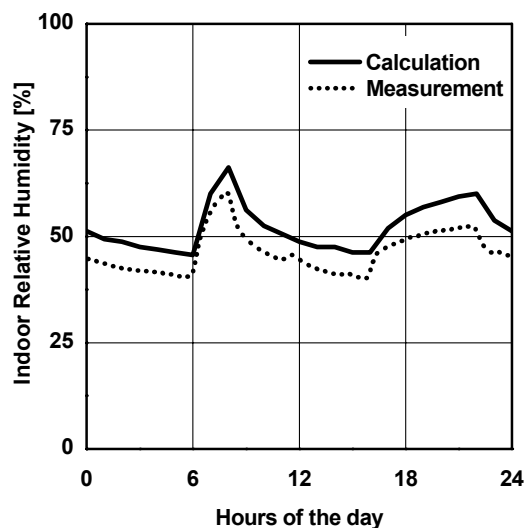


Figure 9 shows the same results for the reference room with the plastered envelope. Again there is a rather good agreement between experiment and calculation, however with a minor offset which is due to a slight difference in the conditions at the beginning of the day. It is assumed that the moisture buffering effect of the envelope retards the dynamic equilibrium in the experiment. This leads to a slightly lower initial RH but does not influence the humidity fluctuations a great deal. The maximum increase in air humidity takes place again in the morning hours but with ca. 20% RH it is considerably lower than in the case of the aluminium foiled test room. This demonstrates the great influence of the vapour absorption capacity of the building envelope.

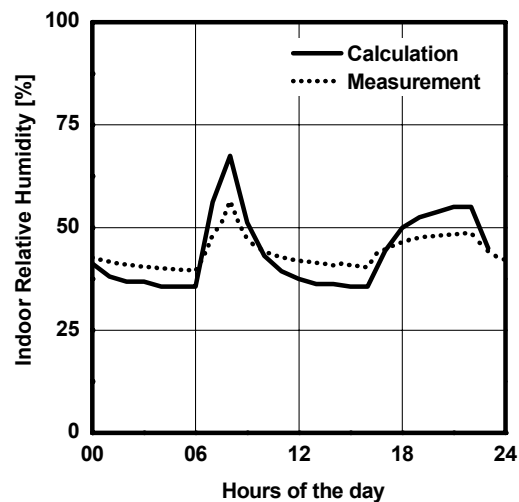
Figure 9: Simulated and measured evolution of the indoor air humidity during a diurnal cycle in the reference room coated with a lime-gypsum interior plaster.



After the initial tests the aluminium foiled test room was lined with wooden panels in order to increase its moisture buffering capacity. Apart from the outdoor climate which was only slightly different all other boundary conditions

were left unchanged. The resulting indoor air humidity evolutions are plotted in *Figure 10*. The measured curve shows very limited humidity fluctuations. The maximum increase in the morning hours is less than 20% which means that the wooden panels have a greater moisture buffering capacity than the unpainted interior plaster. However, this is not captured by the simulated curve which clearly deviates from the measured one. Apparently the hygrothermal properties for wood in the database which were determined by steady state laboratory tests do not represent the transient diffusion and absorption characteristics of the panel surfaces. This effect which has been described by [Hakansson 1998] as non-fickian behaviour must probably be taken into account in order to get a better agreement between simulation and experiment in the case of wood based building envelope materials.

Figure 10: Simulated and measured evolution of the indoor air humidity during a diurnal cycle in the test room when walls and ceiling were covered with wooden panels.



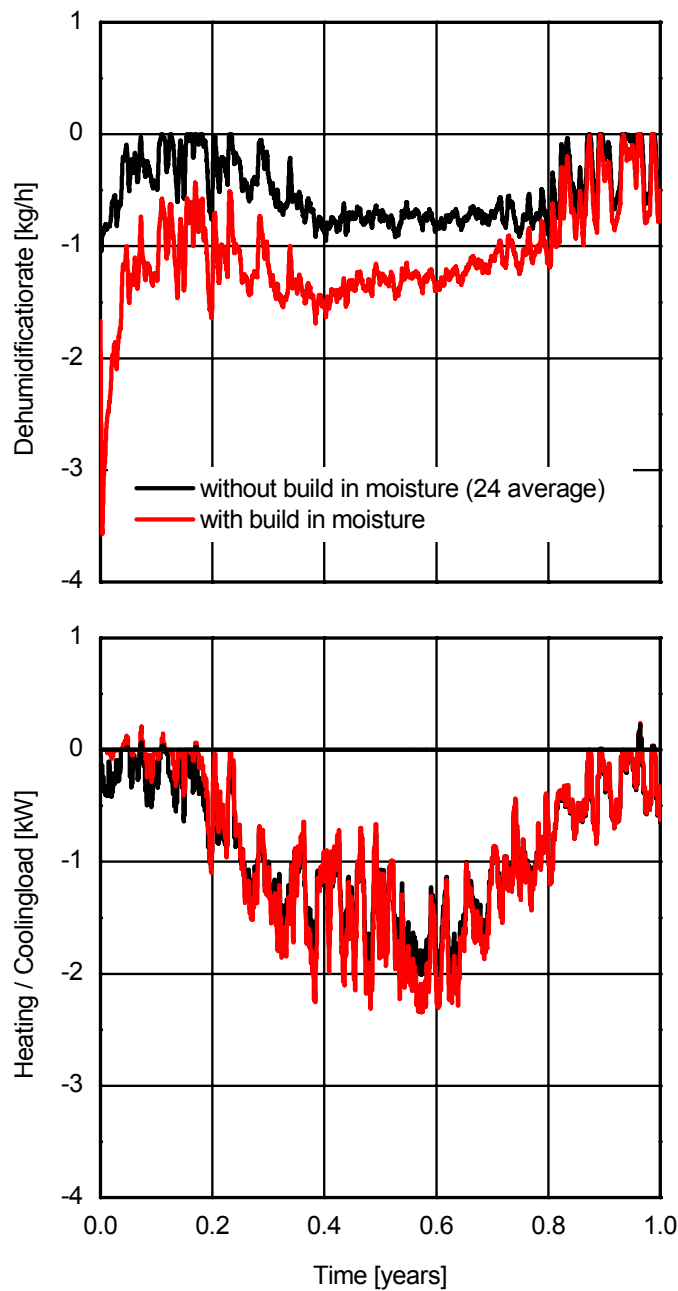
6 Model application

As an application case the hygrothermal behaviour of a 100 m² and 2.5 m high dwelling with a 20 cm thick AAC flat roof and 20 cm thick AAC wall elements will be shown for a period of one year. The roof is sealed from outside with a vapour tight bituminous membrane. On the interior surface a gypsum plaster with a s_d -value of 0.1 m is applied. At the facades a lime cement plaster is applied. On the interior surface a gypsum plaster is applied. On the south-orientated façade windows with a total area of 8 m² and all other orientations with 5 m² each are integrated. Hourly weather data measured for a typical year in Miami (USA) represent the climatic conditions for a hot and humid climate. It is assumed, that the room is occupied from 8 a.m. to 7 p.m. During this time the minimum allowed temperature is 20°C (otherwise 16 C), the moisture production rate in the room is 0.5 kg/h and the internal sources are 2 kW. The comfortable range for the interior RH lies between 40 and 60 %. The maximum allowed temperature is 25 °C. The results are compared for a dwelling with and without construction moisture. The heat transfer coefficient

at the external surface is $17 \text{ W/m}^2\text{K}$, and $8 \text{ W/m}^2\text{K}$ on the inside. The short-wave absorption coefficient of the bituminous felt is 0.6. Rainwater absorption is neglected. The starting point is the beginning of April with an initial moisture content of 20 vol.% in the roof element.

The results give information on the required energy consumption for keeping comfortable climate conditions. Here the necessary dehumidification rate and the heating respectively cooling rate *Figure 11* shows the resulting dehumidification rate for both cases. In order to smooth the results only 24 hour averages are plotted in this graph. Due to the very high construction moisture content (20 Vol.-%) of the AAC elements, the dehumidification rate during the first 10 months is nearly twice as high as in the case without construction moisture. The corresponding cooling load is shown in the same picture at the bottom. The difference between both cases is not as pronounced. The cooling rate is mainly influenced by the exterior conditions. The influence of construction moisture is marginal. Only during the first two months the cooling rate is lower for the dwelling with construction moisture.

Figure 11:
Dehumidification
rate and heating res.
cooling rate (24 h
averages) for the
dwelling during the
first year.



For the first year an average of 7680 kWh is need for cooling if construction moisture is taken into account. This is about 5 % less than in a later stage of the service life of a building (dry construction). This can be explained by the effect of surface cooling due to evaporation during the drying of the AAC elements. On the other hand the construction moisture leads to an annual dehumidification rate of about 9250 kg water, which is nearly twice as high as in the dry case. The consequences are, that if the HVAC system is only designed for the "dry" state of the dwelling, the surplus moisture during the first years can cause problems.

7 Conclusions

The hygrothermal behaviour of the building envelope has an important effect on the overall performance of a construction. Therefore, a combined tool for hygrothermal envelope calculations and whole building simulations has been developed and first steps to validate the model have been successfully completed. The results are promising but many more validation examples are necessary in order to gain confidence in the new model and enhance its performance. Since there are some building materials that react differently when exposed to transient instead of steady state conditions more appropriate hygrothermal parameters may have to be determined for hygrothermal building performance calculations.

Models like the one presented here will help to improve energy simulations because latent heat loads and their temporal pattern can be calculated more accurately. At the same time the determination of indoor air and surface conditions in a building becomes more reliable. This is very important to assess indoor air comfort and hygiene. Post processing models for the determination of mould growth [Sedlbauer 2001] or corrosion risks rely on accurate results of the transient temperature and humidity conditions. The same holds for the design of HVAC systems in heritage buildings or museums [Harriman et al. 2001] where the humidity buffering capacity of the envelope and furniture helps to control temperature and humidity fluctuations.

8 References

Håkansson, H. 1998. *Retarded Sorption in Wood*. Report TABK-98/1012. Sweden: Lund Institute of Technology.

Harriman, L., Brundrett, G. & Kittler, R. 2001. *Humidity Control Design Guide for Commercial and Institutional Buildings*. Atlanta: ASHRAE publication.

Holm, A., Künzle, H. M. & Sedlbauer, K. 2003. *The Hygrothermal Behaviour of Rooms: Combining Thermal Building Simulation and Hygrothermal Envelope Calculation*: IBPSA Proceedings Building Simulation Eindhoven.

Karagiozis, A. & Salonvaara, M. 2001. Hygrothermal system-performance of a whole building. *Building and Environment* 36, vol. 6: 779-787.

Künzle, H. 1984. Heat transmission through the enclosing skin of the building compared with calculated k-value in relation to the wall design. *ZI* (1984), H. 2: 59-65.

Künzel, H. M. 1994. *Simultaneous Heat and Moisture Transport in Building Components. Dissertation.* Stuttgart: University of Stuttgart, Download: www.building-physics.com.

Rode, C., Grau, K., & Mitamura, T. 2001. *Model and Experiments for Hygrothermal Conditions of the Envelope and Indoor Air of Buildings.* Buildings VIII. Clearwater Beach.

Sedlbauer, K.: *Prediction of mould fungus formation on the surface of and inside building components. Dissertation.* University of Stuttgart 2001 , Download: www.building-physics.com.

Trechsel, H.R. et al. 2001. *Moisture Analysis and Condensation Control in Building Envelopes.* West Conshohocken PA, U.S.A.: ASTM MNL40.